The Journal of Chemical Physics

RESEARCH ARTICLE | MAY 25 2023

CASPT2 study of the electronic structure and photochemistry of protonated *N*-nitrosodimethylamine (NDMA-H$^+$) at 453 nm

Juan Soto ; Daniel Peláez ; Manuel Algarra

J. Chem. Phys. 158, 204301 (2023)
https://doi.org/10.1063/5.0147631

AIP Publishing

The Journal of Chemical Physics ARTICLE scitation.org/journal/jcp

CASPT2 study of the electronic structure and photochemistry of protonated *N*-nitrosodimethylamine (NDMA-H$^+$) at 453 nm

Cite as: J. Chem. Phys. 158, 204301 (2023); doi: 10.1063/5.0147631
Submitted: 24 February 2023 • Accepted: 16 May 2023 •
Published Online: 25 May 2023

Juan Soto,[1,a] Daniel Peláez,[2] and Manuel Algarra[3]

AFFILIATIONS

[1] Department of Physical Chemistry, Faculty of Science, University of Málaga, Andalucía Tech., E-29071 Málaga, Spain
[2] Institut des Sciences Moléculaires D'Orsay (ISMO) - UMR 8214., Université Paris-Saclay, 91405 Saclay, Orsay Cedex
[3] INAMAT^2-Institute for Advanced Materials and Mathematics, Departamento de Ciencias, Universidad Pública de Navarra, Campus de Arrosadía, 31006 Pamplona, Spain

[a] **Author to whom correspondence should be addressed:** soto@uma.es

ABSTRACT

In this work, we have studied the photodissociation of the protonated derivatives of *N*-nitrosodimethylamine [$(CH_3)_2N$–NO] with the CASPT2 method. It is found that only one of the four possible protonated species of the dialkylnitrosamine compound absorbs in the visible region at 453 nm, that is, *N*-nitrosoammonium ion $[(CH_3)_2N\mathbf{H}\text{-NO}]^+$. This species is also the only one whose first singlet excited state is dissociative to directly yield the aminium radical cation $[(CH_3)_2NHN\cdot]^+$ and nitric oxide. In addition, we have studied the intramolecular proton migration reaction $\{[(CH_3)_2N\text{–NO}\mathbf{H}]^+ \rightarrow [(CH_3)_2N\mathbf{H}\text{–NO}]^+\}$ both in the ground and excited state (ESIPT/GSIPT); our results indicate that this process is not accessible neither in the ground nor in the first excited state. Furthermore, as a first approximation, MP2/HF calculations on the nitrosamine–acid complex indicate that in acidic solutions of aprotic solvents, only $[(CH_3)_2N\mathbf{H}\text{–NO}]^+$ is formed.

I. INTRODUCTION

Nitrosamines (R_2N–NO) are interesting compounds from both theoretical[1] and practical[1,2] points of view. For example, they are potentially carcinogenic species[3] that have been shown to be ubiquitous, and they can be found in tobacco smoke, food, and even in drinking water[4] On the other hand, they are widely used in synthetic organic chemistry as a source of aminium radical cations (R_2HN^+) because they participate in C–N bond forming reactions with arenes and alkenes.[2] While the mechanism of the gas phase photolysis is relatively simple—the first step yields dimethylamino radical [$(CH_3)_2N$] and nitric oxide (NO)—the photolysis in acidic solution shows a more complicated mechanism, which depends on several factors, such as concentration of nitrosamine, nature of the solvent (protic or aprotic), or the particular acidic species used in the experiments.[4]

Thus, as an archetypical example of *N*-alkylnitrosamines, we have focused our attention on N-nitrosodimethylamine, whose photochemistry, pioneered by Chow and co-workers,[1,5–9] has been studied by many authors both in the gas phase and in acidic solutions.[2,4] A main concern in the photochemistry of NDMA, in acid solution, is the species that participates in the process, that is, it is not clear whether it is nitrosamine (NDMA),[4] the nitrosamine/acid complex (NDMA/HA),[4–6,10] or the protonated nitrosamine (NDMAH$^+$).[1,4] For example, as Beard and Swager[4] pointed out, although it is plausible that the nitrosamine/HA complexes are involved in the photolysis of nitrosamine in aprotic solvents in the presence of an acid, the role of the nitrosamine/HA complex is unclear in alkaline or neutral aqueous solutions, wherein the nitrosamine is predominantly engaged in hydrogen bonding with water or hydronium cation (H_3O^+).

In the context of chemical synthesis, it is only until very recently that the generation of aminium radical species ($NHNO^+$) from *N*-nitrosoamines in acidic solution has been disclosed for the first time through excitation at 453 nm,[11,12] which represents a photosynthetic route for the generation of such radical

species under mild, safe, and simple operationally experimental conditions.[12]

Curiously, little attention has been focused on the theoretical study of the photochemistry of nitrosamines, and even fewer reports using multiconfigurational methods are reported in the literature,[13–15] as demands the extensive electron delocalization of both the NN and NO bonds.[13–17] Therefore, in this work, we have undertaken the theoretical study of the photolysis of NDMA and their protonated derivatives, paying special attention to the photolysis at visible wavelengths (~453 nm). To this end, since the electronic structure of the nitroso compounds demand the application of methods based on multiconfigurational wavefunctions, we have used the CASPT2 approximation.

II. METHODS OF CALCULATION

The complete active space self-consistent field (CASSCF)[18–24] and the multi-state second-order perturbation (MS-CASPT2)[25,26] methods have been applied as implemented in the MOLCAS 8.4 and OpenMOLCAS 22.06 programs.[27–30] MS-CASPT2 energies have been calculated for the CASPT2-optimized geometries. Extended relativistic basis sets of the atomic natural orbital (ANO)-type, that is, ANO-RCC basis sets,[31,32] have been used throughout this work by applying the (C,N,O)[4*s*3*p*2*d*1*f*]/(H)[3*s*2*p*1*d*] contraction scheme. The IPEA empirical correction has been fixed at 0.25 in all of the MS-CASPT2 calculations; equally, to avoid the inclusion of intruder states in such calculations, an imaginary shift set to 0.1 has been applied. Conical intersections have been optimized with the algorithm[33] implemented in MOLCAS. When CASSCF has been applied with the state average approximation, the notation SA*n*-CASSCF has been used, where *n* denotes the number of states of a given symmetry included in the calculation. CASPT2 calculations (geometry and excitation energies), including the solvent effect, have been performed with the polarizable continuum model (PCM).[34,35]

The active space consists in 16 electrons distributed in 14 orbitals, hereafter represented as (16e, 14o; Fig. 1). Unless otherwise indicated, given that the geometry of the electronic ground state of NDMA has been experimentally determined to be planar (C_s symmetry),[36,37] these SA-CASSCF calculations have been performed under such a symmetry point group. The molecular orbitals included in the active space of the CASSCF reference wavefunctions, of the neutral species [NDMA, Fig. 2(a)] and *N*-nitrosoammonium ion [$NHNO^+$, Fig. 2(e)], are represented in Fig. 1. These orbitals have been carefully selected to avoid unrealistic description of both excitation energies and dissociation profiles.[38–40]

Nitrosamine–acid complexes have been optimized with the Møller–Plesset method[41] in conjunction with def2-TZVPP basis sets.[42,43]

The analysis of molecular geometries and molecular orbitals has been performed with the programs Gabedit[44] and Molden,[45] while the analysis of vibrational normal modes have been performed with MacMolplt.[46] Construction of the 1D-potential energy curves (PECs) has been performed by applying a linear interpolation method that uses the full space of non-redundant internal coordinates, as explained in other works.[47–50]

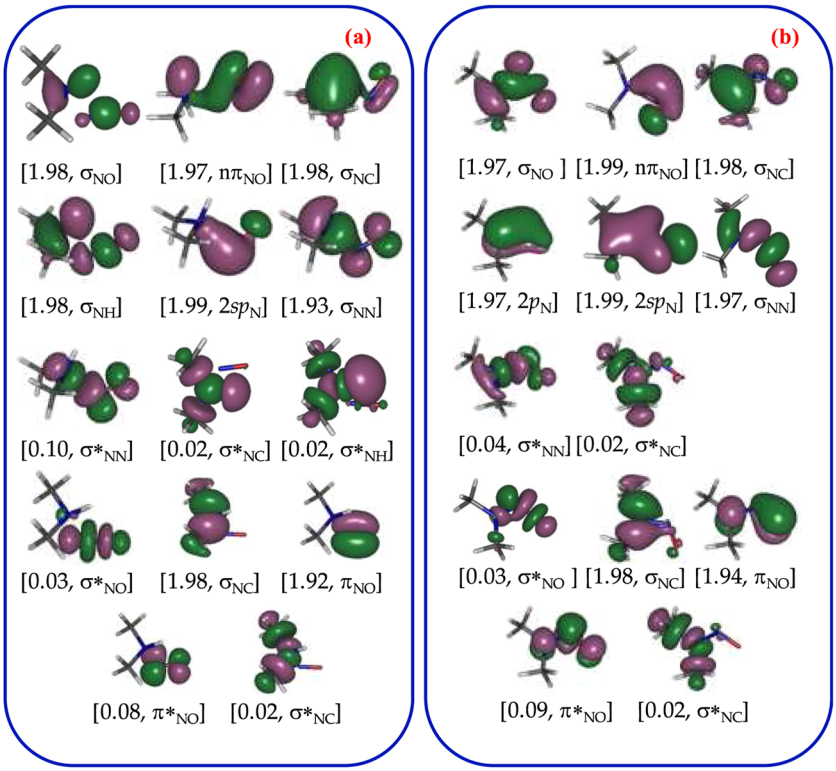

FIG. 1. CASSCF/ANO-RCC orbitals included in the active space of the ground states of (a) *N*-nitrosoammonium ion and (b) *N*-nitrosodimethylamine. Square brackets: occupation numbers.

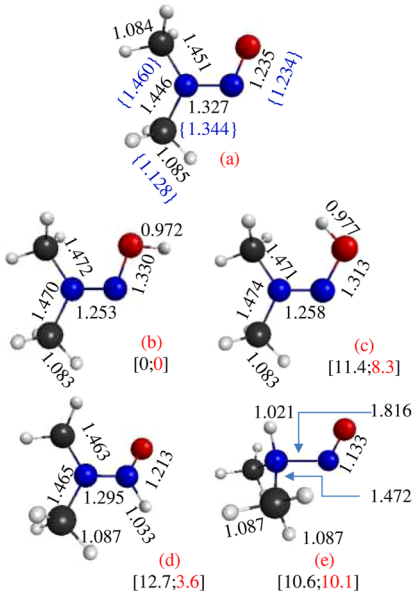

FIG. 2. CASPT2/ANO-RCC optimized geometries of (a) *N*-nitrosodimethylamine [NDMA], (b) *E*-protonated *N*-nitrosodimethylamine [*E*-$NNOH^+$], (c) *Z*-protonated *N*-nitrosodimethylamine [*Z*-$NNOH^+$], (d) N-protonated *N*-nitrosodimethylamine [$NN\,H^+O$], and (e) *N*-nitrosoammonium ion [NH^+NO]. Square brackets: relative energies in kcal/mol of the protonated nitrosamines with respect to *E*-$NNOH^+$. Curly brackets: experimental parameters from gas phase electron diffraction (Refs. 36 and 37). Red: relative electronic energies of the tautomers, including the solvent effect (methanol, PCM).

III. RESULTS AND DISCUSSION

A. Relative energies of protonated *N*-nitrosodimethylamines

In this section, prior to describing the photodissociation of *N*-nitrosodimethylamine, we study the excitation properties of neutral *N*-nitrosodimethylamine and four of their protonated isomers (Fig. 2).

The geometries represented in Fig. 2 correspond to the CASPT2 optimized geometries of the isolated species. Along with the main structural parameters (descriptions and values of full internal coordinates are given in Table SIa), we have included the relative electronic energies in kcal/mol of the protonated species in Fig. 2, with and without inclusion of solvent effect. For protonated *N*-nitrosodimethylamine, we give in Table SIb the parameters that are obtained after including the solvent effect in the geometrical optimization. Protonation of nitrosamine involves, with respect to the neutral molecule, lengthening of the N–O bond and shortening of the N–N bond, excepting for the *N*-nitrosoammonium ion [Fig. 2(e)], wherein we have found the reverse effect, that is, an unusual elongation of the N–N bond (~0.5 Å) and shortening of the N–O internuclear distance. However, it must be remarked that, as will be discussed in Sec. III D, the ammonium ion is a molecule bonded by covalent unions and is not van der Waals type adduct. The most stable isomer corresponds to *E*-$NNOH^+$ [Fig. 2(b)], which is the species generally assumed to be formed as the initial protonated isomer.

The main thermodynamics properties of the protonated molecules represented in Fig. 2 are listed in Table I, which have been estimated with the standard expressions of statistical thermodynamics. This table includes both the properties of the isolated and solvated species. In accordance with the data presented in Table I, it could be argued that the $NHNO^+$ tautomer will only be present in negligible amounts because the equilibrium of the *E*-$NNOH^+ \leftrightharpoons NHNO^+$ reaction is displaced in the direction of the *E*-$NNOH^+$. However, the actual equilibrium must be established as *Z*-$NNOH^+ \leftrightharpoons NHNO^+$ through the transition state **TS1** [*vide infra*, Fig. 4(c)] and whose barrier height is 60 kcal/mol. Furthermore, there exists a conical intersection [*vide infra*, **CI1** Figs. 4(b) and 4(e)], which is positioned just in the reaction path of the *Z*-$NNOH^+ \leftrightharpoons$ *E*-$NNOH^+$ tautomerization and hinders, if not forbids, such an equilibrium. This "passive" effect of the conical intersection corresponds to the so-called "diabatic trapping" case, which involves non-diabatic recrossing of the potential energy surfaces.[51–58] Therefore, the formation and concentration of $NHNO^+$ is not kinetically nor thermodynamically controlled by its *E*-$NNOH^+$ tautomer. It must be remarked that this unfavorable 1,3 hydrogen transfer could be drastically reduced if a protic solvent assists the proton transfer.

Since the species represented in Fig. 2 are not expected to be found as isolated species in solution, we have studied the complexes formed by NDMA with hydronium ion (H_3O^+) or methanesulfonic acid (MsOH); the later complexes would correspond to those formed in the experiments in non-aqueous, aprotic solvents.[11,12] It must be remarked that the calculations of these complexes must be understood as a model first approximation. The MP2/RHF geometries of three of the possible complexes of NDMA/H_3O^+ and NDMA/MsOH, respectively, are depictured in FIG. S1, where the obtained results for both gas-phase and solution in three organic solvents are included. The interaction of NDMA with H_3O^+ leads to proton transfer from the hydronium anion to NDMA, forming $NDMAH^+/H_2O$ complexes analogous to the protonated species included in Fig. 2. Remarkably, proton transfer from MsOH to NDMA (the acid used in the works of Oh *et al.*[11,12]) only occurs when the analogous complex to the *N*-nitrosoammonium ion ($NHNO^+$) is formed, that is, $NHNO^+/MsO^-$ (FIG. SIf), which supports the central idea of this work, that is, the reactive species is NH^+NO. The geometrical and energetics parameters of the calculations performed on these complexes for the isolated species and with inclusion of solvent effect (methanol, dimethylsufoxide, and acetonitrile) are given in the supplementary material.

B. Excited states and photodissociation of protonated *N*-nitrosodimethylamines

As a first stage, we have calculated the singlet vertical excitation energies of the molecules at the MS-CASPT2 level using a SA2-CASSCF(16e, 14o) reference wavefunction (Tables II and III).

Table II includes the calculated vertical excitations of the five molecular species represented in Fig. 2, calculated as isolated molecules. The most remarkable feature of the data collected in Table II is that the only species that absorbs in the visible region of the spectrum (453 nm) is the *N*-nitrosoammonium ion [$NHNO^+$, Fig. 2(e)], the unique species that is protonated with MsOH

TABLE I. Thermodynamics properties of protonated *N*-nitrosodimethylamines in kcal/mol with respect to *E*-$NNOH^+$.[a]

Species	ΔU (0)	ΔH (298.15 K)	ΔG (298.15 K)
		Gas phase	
$NHNO^+$	9.2	9.8	7.8
Z-$NNOH^+$	11.1	11.1	11.1
NNH^+O	13.0	13.1	12.7
		Solution (methanol)	
NH^+NO	8.4	9.0	7.0
Z-$NNOH^+$	6.6	7.2	5.3
NNH^+O	3.5	3.6	3.2

[a]Calculated with standard expressions of statistical thermodynamics: electronic and geometrical parameters (CASPT2) and frequencies (CASSCF).

TABLE II. MS-CASPT2 vertical excitation energies (ΔE) in eV (nm) of nitrosodimethylamines.

Species	State	ΔE	f^l_{OSC}[a]	f^v_{OSC}[b]	*configuration*[c]	W[d]
NMDA[e]	1A″	3.52 (352)	$3.61\ 10^{-3}$	$8.17\ 10^{-3}$	$(\sigma_{NO})^1(\pi^*_{NO})^1$	86
	2A′	5.73 (216)	$2.18\ 10^{-1}$	$2.03\ 10^{-1}$	$(\pi_{NN})^1(\pi^*_{NO})^1$	82
	2A″	7.75 (160)	$9.54\ 10^{-3}$	$9.06\ 10^{-3}$	$(\sigma_{NO})^1(\pi_{NO})^1(\pi^*_{NO})^2$	19
					$(2sp_N)^1(\pi^*_{NO})^1$	69
E-NNOH$^+$[,f]	1A″	5.59 (222)	$8.85\ 10^{-3}$	$8.34\ 10^{-3}$	$(\sigma_{NN})^1(\pi^*_{NO})^1$	69
					$(\sigma_{NC})^1(\pi^*_{NO})^1$	17
	2A′	6.60 (188)	$2.41\ 10^{-1}$	$2.34\ 10^{-1}$	$(\pi_{NNO})^1(\pi^*_{NO})^1$	85
	2A″	9.29 (134)	$1.15\ 10^{-4}$	$7.70\ 10^{-4}$	$(\sigma_{NN})^1(\pi^*_{NO})^1$	19
					$(\sigma_{NC})^1(\pi^*_{NO})^1$	64
Z-NNOH$^+$[,f]	1A″	5.93 (209)	$1.82\ 10^{-2}$	$1.44\ 10^{-2}$	$(\sigma_{NN})^1(\pi^*_{NO})^1$	43
					$(\sigma_{NC})^1(\pi^*_{NO})^1$	47
	2A′	6.55 (189)	$2.49\ 10^{-1}$	$2.50\ 10^{-1}$	$(\pi_{NNO})^1(\pi^*_{NO})^1$	85
	2A″	8.29 (150)	$2.36\ 10^{-4}$	$4.98\ 10^{-4}$	$(\sigma_{NN})^1(\pi^*_{NO})^1$	47
					$(\sigma_{NC})^1(\pi^*_{NO})^1$	42
NNHO$^+$[,f]	1A″	4.16 (298)	$2.37\ 10^{-4}$	$2.56\ 10^{-4}$	$(\sigma_{NC})^1(\pi^*_{NO})^1$	19
					$(2sp_N)^1(\pi^*_{NO})^1$	66
	2A′	5.71 (217)	$2.75\ 10^{-1}$	$2.80\ 10^{-1}$	$(n\pi_N)^1(\pi^*_{NO})^1$	80
	2A″	9.21 (135)	$6.75\ 10^{-4}$	$5.55\ 10^{-4}$	$(\sigma_{NC})^1(\pi^*_{NO})^1$	56
					$(2sp_N)^1(\pi^*_{NO})^1$	22
NHNO$^+$[,f]	1A″	2.74 (453)	$6.31\ 10^{-4}$	$1.10\ 10^{-3}$	$(\sigma_{NN})^1(\pi^*_{NO})^1$	84
	2A′	6.43 (193)	$4.62\ 10^{-1}$	$4.79\ 10^{-1}$	$(\pi_{NO})^1(\pi^*_{NO})^1$	80
	2A″	8.19 (151)	$3.38\ 10^{-3}$	$2.46\ 10^{-3}$	$(\sigma_{NN})^1(\pi_{NO})^1(\pi^*_{NO})^2$	12
					$(\sigma_{NO})^1(\pi^*_{NO})^1$	65

[a]Oscillator strength (length formula).
[b]Oscillator strength (velocity formula).
[c]MS-CASPT2 main electronic configurations of the excited states referred to the ground state configuration.
[d]Weight of the configuration in %. Only contributions greater than 10% are included.
[e]Reference wave function 1: SA2-CASSCF(16,13)/ANO-RCC (**C,N,O**[4s3p2d1f]/**H**[3s2p1d]).
[f]Reference wave function 2: SA2-CASSCF(16,14)/ANO-RCC (**C,N,O**[4s3p2d1f]/**H**[3s2p1d]).

TABLE III. MS-CASPT2 vertical excitation energies (ΔE) in eV (nm) of protonated *N*-nitrosodimethylamines. Transition energies and ground state CASPT2 optimized geometries including the solvent effect (PCM, methanol).[a]

Species	State	ΔE	f^{l}_{OSC}[b]	f^{v}_{OSC}[c]	*configuration*[d]	*W*[e]
E-NNOH$^+$	1A″	5.62 (221)	$8.72\ 10^{-3}$	$8.14\ 10^{-3}$	$(\sigma_{NN})^1(\pi^*_{NO})^1$	71
					$(\sigma_{NC})^1(\pi^*_{NO})^1$	16
	2A′	6.53 (190)	$2.45\ 10^{-1}$	$2.35\ 10^{-1}$	$(\pi_{NNO})^1(\pi^*_{NO})^1$	85
	2A″	9.31 (133)	$3.93\ 10^{-4}$	$2.54\ 10^{-4}$	$(\sigma_{NN})^1(\pi^*_{NO})^1$	19
					$(\sigma_{NC})^1(\pi^*_{NO})^1$	65
Z-NNOH$^+$	1A″	5.99 (207)	$1.82\ 10^{-2}$	$1.47\ 10^{-2}$	$(\sigma_{NN})^1(\pi^*_{NO})^1$	40
					$(\sigma_{NC})^1(\pi^*_{NO})^1$	50
	2A′	6.59 (188)	$2.50\ 10^{-1}$	$2.50\ 10^{-1}$	$(\pi_{NNO})^1(\pi^*_{NO})^1$	85
	2A″	8.31 (149)	$2.25\ 10^{-4}$	$5.11\ 10^{-4}$	$(\sigma_{NN})^1(\pi^*_{NO})^1$	43
					$(\sigma_{NC})^1(\pi^*_{NO})^1$	47
NNHO$^+$	1A″	4.29 (289)	$3.39\ 10^{-4}$	$3.65\ 10^{-4}$	$(\sigma_{NC})^1(\pi^*_{NO})^1$	25
					$(2sp_N)^1(\pi^*_{NO})^1$	62
	2A′	5.75 (216)	$2.85\ 10^{-1}$	$2.94\ 10^{-1}$	$(n\pi_N)^1(\pi^*_{NO})^1$	82
	2A″	9.14 (136)	$2.21\ 10^{-4}$	$2.92\ 10^{-4}$	$(\sigma_{NC})^1(\pi^*_{NO})^1$	55
					$(2sp_N)^1(\pi^*_{NO})^1$	28
NHNO$^+$	1A″	2.72 (456)	$7.36\ 10^{-4}$	$1.47\ 10^{-3}$	$(\sigma_{NN})^1(\pi^*_{NO})^1$	86
	2A′	6.90 (180)	$3.72\ 10^{-1}$	$4.03\ 10^{-1}$	$(\pi_{NO})^1(\pi^*_{NO})^1$	81
	2A″	7.93 (156)	$4.49\ 10^{-3}$	$3.47\ 10^{-3}$	$(\sigma_{NN})^1(\pi_{NO})^1(\pi^*_{NO})^2$	14
					$(\sigma_{NO})^1(\pi^*_{NO})^1$	68

[a]Reference wave function: SA2-CASSCF(16,14)/ANO-RCC (**C,N,O**[4s3p2d1f]/**H**[3s2p1d]).
[b]Oscillator strength (length formula).
[c]Oscillator strength (velocity formula).
[d]MS-CASPT2 main electronic configurations of the excited states referred to the ground state configuration.
[e]Weight of the configuration in %. Only contributions greater than 10% are included.

(FIG. SIf). This observation would correspond to the conditions in which the experiments of Patil and co-authors are conducted with aprotic solvents.[11,12] The excitation at 453 nm corresponds to a $\sigma_{NN} \rightarrow \pi^*_{NO}$ electronic transition, which weakens the σ(N–N) bond [Fig. 1(a)] and suggests that it would lead to dissociation of $NNHO^+$ into $(CH_3)_2N^+$ and NO. Two approximations, length and velocity formulas, have been applied to the calculation of oscillator strengths, which would only be coincident when computed with the true wave functions.[59] In addition, for the sake of completeness, geometry optimization of protonated tautomers, excitation energies, and oscillator strengths have been computed as well, including the solvent effect with the PCM approximation, and the results are listed in Table III for methanol as the solvent; the results obtained when the solvents are dimethylsulfoxide or acetonitrile (the other two solvents used by Patil and co-authors[12]) are listed in Table SII, where it can be observed that there is no significant difference among calculated properties in changing the solvent.

The potential energy profiles of the nitrosamines studied in this work that lead to N–N bond breaking are represented in Fig. 3, where the main varying coordinate is the N–N internuclear distance. In addition, with the purpose of comparing reactivity of related nitrosamines, we have included the dissociation paths of the smallest protonated nitrosamine ($[NH_3NO]^+$), which was studied in a previous work.[14] From the inspection of the electronic configurations of the singlet states at the last step (dissociated molecule) of each interpolation curve represented in Fig. 3, we have found that the only two species that yield NO (nitric oxide) are neutral nitrosodimethylamine [NDMA, Fig. 3(a)] and *N*-nitrosoammonium ion [$NHNO^+$, Fig. 3(e)]; *Z*- and *E*-NNOH+ give NOH^+ [cation of the hyponitrous acid monomer, Figs. 3(b) and 3(c)]; $NNHO^+$ generates the cation of nitroxyl [HNO^+, Fig. 3(d)]. It must be noted that NH_3NO^+ yields the cation of nitric oxide [NO^+, Fig. 3(f)]. Another important feature that must be remarked on Fig. 3 is that the only dissociative potential energy surface corresponds to the S_1 state of $NHNO^+$ [Fig. 3(e)]. Therefore, after absorption of visible light (453 nm), the S_1 excited state of $NHNO^+$ decomposes into NO and $(CH_3)_2N^+$.

Since the experiments of Chow *et al.*[1,13] on the photochemical decomposition of unprotonated nitrosodimethylamine (NDMA) were conducted at 450 nm (63.5 kcal/mol) and explained via direct population of the triplet potential energy surface, we have included the energy profiles of the low-lying triplet states in each one of the interpolations represented of Fig. 3. Accordingly, it can be observed in Fig. 3 that the only protonated tautomer of *N*-nitrosodimethylamines, whose lowest triplet state would be accessible upon irradiation at 453 nm, is the *N*-nitrosoammonium ion

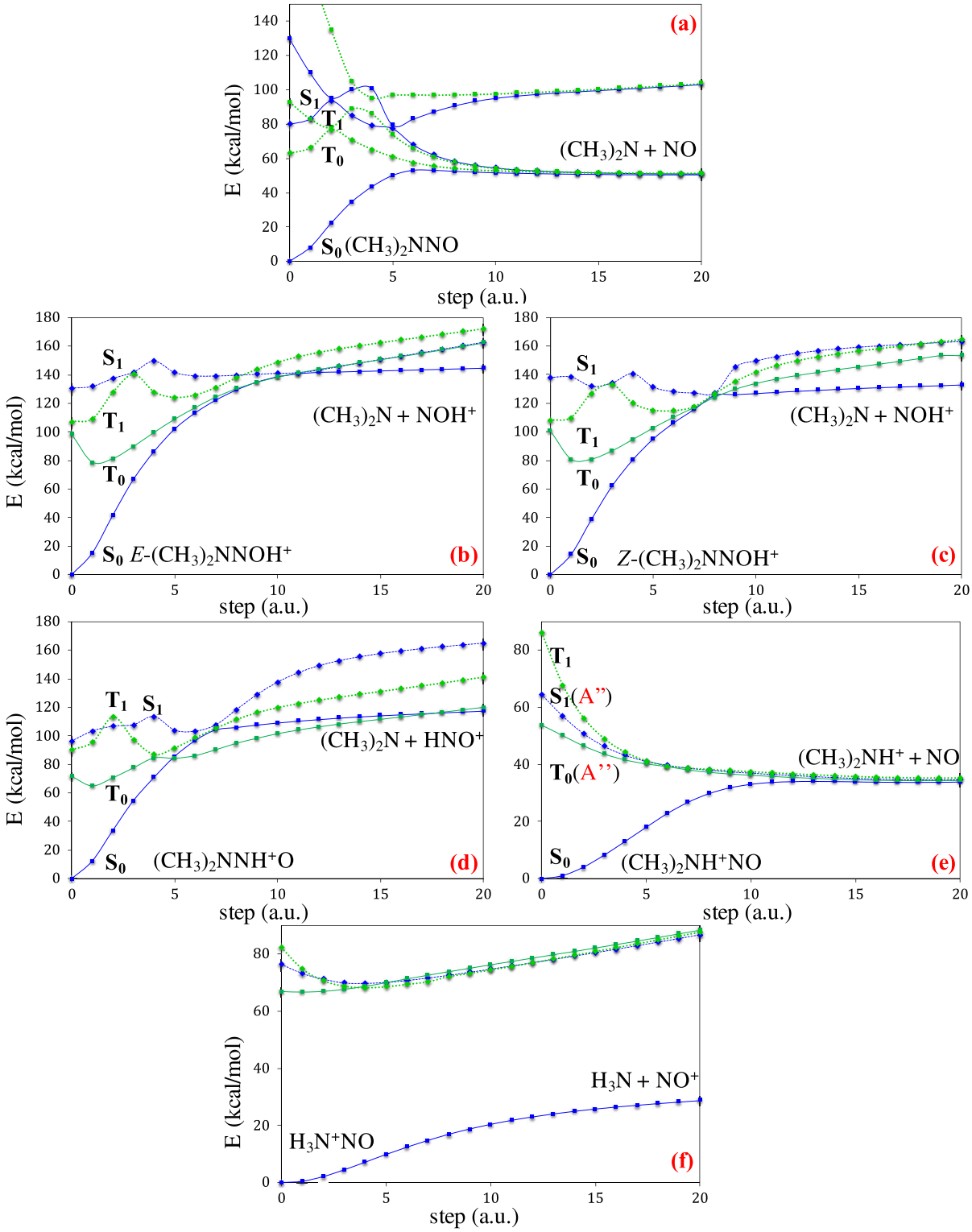

FIG. 3. Potential energy profiles (linear interpolations) of the lowest singlet and triplet states of the dissociation reactions of (a) *N*-nitrosodimethylamine [NDMA], (b) *E*-protonated *N*-nitrosodimethylamine [*E*-NNOH$^+$], (c) *Z*-protonated *N*-nitrosodimethylamine [*Z*-NNOH$^+$], (d) N-protonated *N*-nitrosodimethylamine [NNH$^+$O], (e) *N*-nitrosoammonium ion [NH$^+$NO], and (f) protonated nitrosamine $[NH_3NO]^+$.

[NH^+NO, Fig. 3(e)]. Furthermore, this tautomer is the only one that exhibits a dissociative triplet state (T_0), with energy below the radiation of 453 nm [Fig. 3(e)]. However, given that the $S_0 \rightarrow S_1$ spin allowed transition is in resonance with the 453 nm radiation and is dissociative, population of the triplet state via S_1/T_0 intersystem crossing is very unlikely, especially when the vertical energy of the T_0 state is well below 453 nm, and more importantly, the S_1/T_0 crossing is forbidden by symmetry or El-Sayed's rules[60,61] because both states (S_1 and T_0) belong to A″ symmetry. Thus, it is not necessary to invoke the participation of triplet states via intersystem crossing in the photodissociation of protonated nitrosamines.

C. Excited state intramolecular proton transfer (ESIPT) to form *N*-nitrosoammonium ion ($NHNO^+$)

One of the mechanisms proposed to explain the formation of *N*-nitrosoammonium ion is excited state intramolecular proton transfer (ESIPT).[62–65] That is, it is suggested in previous studies that the *N*-nitrosoammonium cation ($NHNO^+$) is photochemically formed in the excited state from the protonated nitrosamine ($NNOH^+$). Thus, in this section, we have studied proton migration from *Z*-$NNOH^+$ to $NHNO^+$, both in the ground state and first excited state. Figure 4 represents the critical points that would be involved in such reactions. We have found the following critical point on the S_1 surface related to the reaction under study, that is, a first order saddle point on the S_1 surface [**SD1**, Fig. 4(a)] that would lead from *Z*-$NNOH^+$ with $NHNO^+$. However, after analyzing the potential energy surface, we must conclude that this saddle point connects $NHNO^+$ with a S_1/S_0 conical intersection [**CI1**, Fig. 4(b)], and this crossing point, in turn, connects *Z*-$NNOH^+$ with *E*-$NNOH^+$ [Fig. 4(e)]. Furthermore, there are no minima associated with NHNO+, Z-NNOH+, or E-NNOH+ on the S_1 surface. Therefore, proton migration is not a plausible reaction in the excited state; this process would occur in the ground state via the transition state given in [**TS1**, Fig. 4(c)]. The energy profiles for the $NHNO^+$–SD1–Z-$NNOH^+$ paths are represented in Fig. 4(d), and the interconversion Z-$NNOH^+$ ↔ E-ZNNOH+ through CI1 is depictured in Fig. 4(e). The geometrical parameters of species represented in Fig. 4 are listed in Table SIII, and the potential energy curve of proton migration through **TS1** on the ground state surface is represented in FIG. SII.

D. Electronic structure of *N*-nitrosoammonium ion

As mentioned in Subsection I A, the N–N internuclear distance is unusually long in the nitrosoammonium ion [$NHNO^+$,

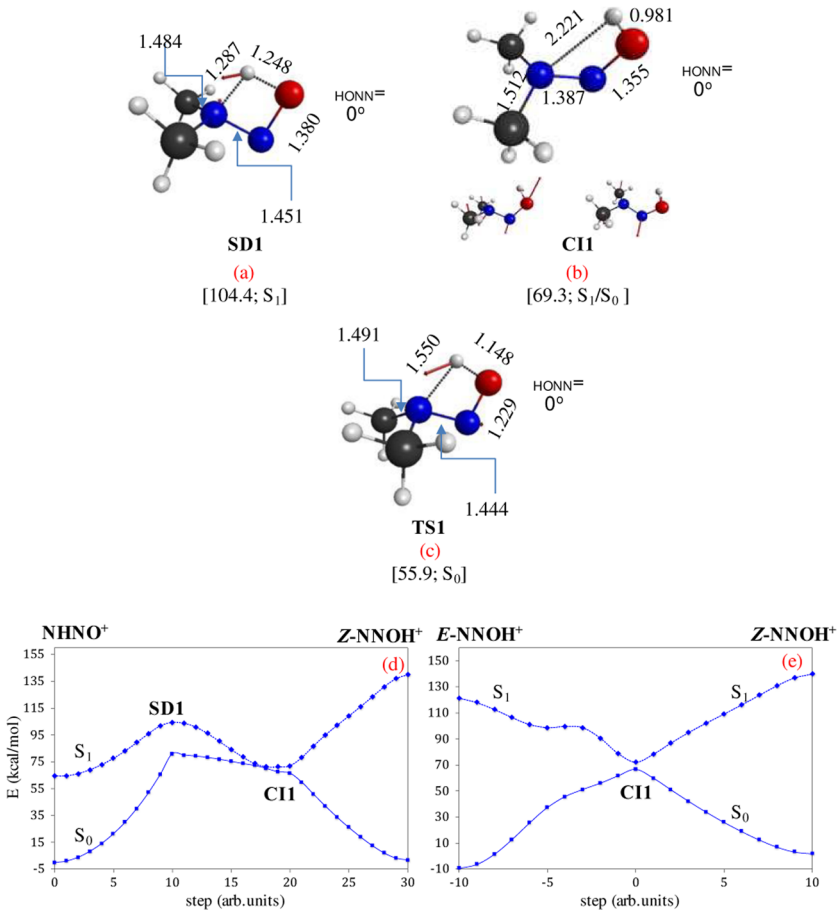

FIG. 4. (a) CASPT2/ANO-RCC optimized geometry of the saddle point (SD1) connecting NH^+NO with conical intersection (CI1) on the S_1 surface. (b) CASSCF/ANO-RCC optimized geometry of the S_1/S_0 conical intersection (CI1) for radiationless deactivation of *E*-$NNOH^+$ to *Z*-$NNOH^+$. (c) CASPT2/ANO-RCC optimized geometry of the transition state (TS1) connecting *E*-$NNOH^+$ with NH^+NO on the S_0 surface. Square brackets: relative electronic energies in kcal/mol with respect to NH^+NO. (d) Energy profiles of the S_1 and S_0 curves going from NH^+NO to Z-$NNOH^+$. (e) Energy profiles of the S_1 and S_0 curves for *E*-$NNOH^+$ ↔ Z-$NNOH^+$ isomerization.

TABLE IV. MS-CASPT2 orbitals of the main configuration state functions of the S_0 state of the *N*-nitrosoammonium ion (NHNO) along the dissociation path [Fig. 3(e)].[a]

Step[b]	OM(σ_{NN})	OM(σ^*_{NN})	$\ldots[\sigma_{NN}]^2[\sigma^*_{NN}]^{0,c}\ldots$	$\ldots[\sigma_{NN}]^1[\sigma^*_{NN}]^{1,d}\ldots$
0	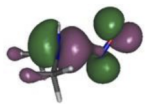	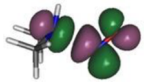	0.92	−0.14
4	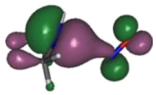	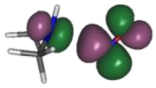	−0.85	0.32
8	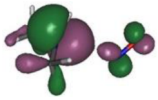	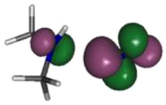	−0.63	0.61
12	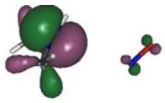	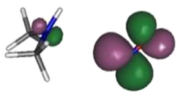	0.29	−0.88
16	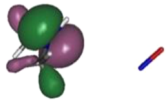	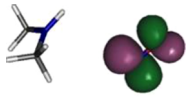	0.10	−0.94
20	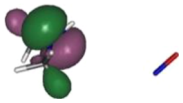	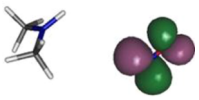	0.	0.95

[a]Reference configuration A′/A″: $[\sigma_{NO}]^2[n\pi_{NO}]^2[\sigma_{NC}]^2[\sigma_{NH}]^2[2sp_N]^2[\sigma_{NN}]^2[\sigma^*_{NN}]^0[\sigma^*_{NC}]^0[\sigma^*_{NH}]^0[\sigma^*_{NO}]^0/[\sigma_{NC}]^2[\pi_{NO}]^2[\pi^*_{NO}]^0[\sigma^*_{NC}]^0$.
[b]Number of step along interpolation.
[c]Coefficient of configuration I.
[d]Coefficient of configuration II.

Fig. 2(e)]. Furthermore, the vibrational analysis of the molecule according to the *GF*-method of Wilson[66,67] yields an exceptional low frequency value of the normal mode associated with N–N stretching [(252 cm^{-1}) Tables SIV and SV], which contrasts with frequency of the neutral nitrosamine (NDMA) that amounts to 1509 cm^{-1} (Tables SVI and SVII). Thus, the purpose of this section is to clarify whether $NHNO^+$ is a van der Waals complex or a covalently bonded compound. To reach this end, we have analyzed the electronic structure (configurations) of the molecule along the S_0 dissociation path previously represented in Fig. 3(e). Given that the most representative configurations along this path only involve excitations within the orbitals associated with the N–N bond (σNN and σ*NN), we have focussed our attention to such orbitals. Table IV collects the variation of the molecular orbitals and coefficients of the two main configuration state functions along the dissociation path. It is clearly observed in Table IV that at the equilibrium geometry of $NHNO^+$, the orbital that describe the σ_{NN} bond is doubly occupied (configuration I) and how its occupancy decays to zero as dissociation progress. In contrast, the occupancy of the σ^*_{NN} bond (configuration II) increases as the dissociation advances. It is observed as well that the character of the initial orbitals changes along the dissociation path; they become from sigma orbital to non-bonding orbitals to give a radical on each fragment. From our opinion, that is the key to classify $NHNO^+$ as a covalently bonded molecule. Otherwise, the biradical character of the molecule should have been observed in the calculations from the beginning at the equilibrium geometry.

IV. CONCLUSIONS

In this work, we have studied the photodissociation of four protonated derivatives of nitrosodimethylamine (NDMA) with the MS-CASPT2 method, both in the gas and solution phases. It is found that the unique protonated derivative species, which absorbs in the visible range of the spectrum, is the *N*-nitrosoammonium ion [Fig. 2(e)], whose S_1 vertical excitation lies at 453 nm. In addition, it is shown that the first excited state of such a derivative is dissociative and yields nitric oxide and aminium radical cation $[(CH_3)_2NHN\cdot]^+$ after photon absorption. The barrier for dissociation into nitric oxide and the radical cation on the ground state amounts to ~34 kcal/mol and is degenerate with S_1 due to degeneration of the ground state of nitric oxide. We have also studied the excited state proton intramolecular migration (ESPIT) for the isomerization of $[Z\text{-}(CH_3)_2N\text{–}NO\mathbf{H}]^+$ to $[(CH_3)_2N\mathbf{H}\text{–}NO]^+$; it is found that this reaction is not plausible in the excited state because the existence of a S_1/S_0 conical intersection that would lead to isomerization of $[Z\text{-}(CH_3)_2N\text{–}NO\mathbf{H}]^+$ to $[E\text{-}(CH_3)_2N\text{–}NO\mathbf{H}]^+$. We have also studied the nature of the N–N bond in the *N*-nitrosoammonium ion; it is found that it is a covalent bond. To finish, in contrast to neutral N-nitrosodimethylamine,[1,7] it is not necessary to invoke the

participation of triplet states (intersystem crossing) in the photodissociation of protonated nitrosamines due to that S1/T0 intersystem crossing is prohibited by El-Sayed's rule.

SUPPLEMENTARY MATERIAL

The supplementary material contains absolute energies, CASSCF molecular orbitals, and internal and Cartesian coordinates of all the critical points.

ACKNOWLEDGMENTS

This work was supported by the Spanish Ministry of Science and Innovation (Grant No. MCIN/AEI/10.13039/501100011033) through Project No. PID2021-122613OB-I00. J.S. thanks Rafael Larrosa, Darío Guerrero, and F. Moreno for the technical support in running the calculations and the SCBI (Supercomputer and Bioinformatics) of the Univ. Málaga for computer and software resources.

AUTHOR DECLARATIONS

Conflict of Interest

The authors have no conflicts to disclose.

Author Contributions

Juan Soto: Investigation (lead); Writing – original draft (lead); Writing – review & editing (lead). **Daniel Peláez**: Investigation (supporting); Writing – original draft (supporting); Writing – review & editing (supporting). **Manuel Algarra**: Investigation (supporting); Writing – original draft (supporting); Writing – review & editing (supporting).

DATA AVAILABILITY

The data that support the findings of this study are available within the article and its supplementary material.

REFERENCES

[1] Y. L. Chow, Z. Z. Wu, M. P. Lau, and R. W. Yip, J. Am. Chem. Soc. **107**, 8196 (1985).
[2] J. M. Ganley, P. R. D. Murray, and R. R. Knowles, ACS Catal. **10**, 11712 (2020).
[3] P. N. Magee and J. M. Barnes, Brit. J. Cancer **10**, 114 (1956).
[4] J. C. Beard and T. M. Swager, J. Org. Chem. **86**, 2037 (2021).
[5] Y. L. Chow, Acc. Chem. Res. **6**, 354 (1973).
[6] Y. L. Chow and Z. Z. Wu, J. Am. Chem. Soc. **107**, 3338 (1985).
[7] Y. L. Chow, Can. J. Chem. **43**, 2711 (1965).
[8] Y. L. Chow, J. Am. Chem. Soc. **87**, 4642 (1965).
[9] Y.-L. Chow, C. J. Colon, and S. C. Chen, J. Org. Chem. **32**, 2109 (1967).
[10] W. S. Layne, H. H. Jaffe, and H. Zimmer, J. Am. Chem. Soc. **85**, 435 (1963).
[11] D. V. Patil, T. Si, H. Y. Kim, and K. Oh, Org. Lett. **23**, 3105 (2021).
[12] D. V. Patil, Y. Lee, H. Y. Kim, and K. Oh, Org. Lett. **24**, 5840 (2022).
[13] D. Peláez, J. F. Arenas, J. C. Otero, and J. Soto, J. Org. Chem. **72**, 4741 (2007).
[14] D. Peláez, J. F. Arenas, J. C. Otero, F. J. Ávila, and J. Soto, J. Phys. Chem. A **112**, 8394 (2008).
[15] D. Peláez, J. F. Arenas, J. C. Otero, and J. Soto, J. Chem. Phys. **125**, 164311 (2006).
[16] J. F. Arenas, J. C. Otero, D. Peláez, and J. Soto, J. Org. Chem. **71**, 983 (2006).
[17] J. Soto, D. Peláez, and J. C. Otero, J. Chem. Phys. **154**, 044307 (2021).
[18] B. O. Roos, in *Advances in Chemical Physics, Ab Initio Methods in Quantum Chemistry II*, edited by K. P. Lawley John Wiley and Sons, Chichester, UK, 1987, Chap. 69, p. 399.
[19] B. O. Roos, P. R. Taylor, and P. E. M. Sigbahn, Chem. Phys. **48**, 157 (1980).
[20] B. O. Roos, Int. J. Quantum Chem. **18**, 175 (1980).
[21] P. E. M. Siegbahn, J. Almlöf, A. Heiberg, and B. O. Roos, J. Chem. Phys. **74**, 2384 (1981).
[22] H. J. Werner and W. Meyer, J. Chem. Phys. **73**, 2342 (1980).
[23] H. J. Werner and W. Meyer, J. Chem. Phys. **74**, 5794 (1981).
[24] J. Olsen, Int. J. Quantum Chem. **111**, 3267 (2011).
[25] B. O. Roos, K. Andersson, M. P. Fülscher, P. A. Malmqvist, L. Serrano-Andrés, K. Pierloot, and M. Merchán, Adv. Chem. Phys. **93**, 219 (1996).
[26] J. Finley, P.-Å. Malmqvist, B. O. Roos, and L. Serrano-Andrés, Chem. Phys. Lett. **288**, 299 (1998).
[27] MOLCAS 8.4 V. Veryazov, P.-O. Widmark, L. Serrano-Andrés, R. Lindh, and B. O. Roos, Int. J. Quantum Chem. **100**, 626 (2004).
[28] MOLCAS 8.4 F. Aquilante, J. Autschbach, R. K. Carlson, L. F. Chibotaru, M. G. Delcey, L. De Vico, I. Fdez. Galván, N. Ferré, L. M. Frutos, L. Gagliardi, M. Garavelli, A. Giussani, C. E. Hoyer, G. Li Manni, H. Lischka, D. Ma, P. Å. Malmqvist, T. Müller, A. Nenov, M. Olivucci, T. B. Pedersen, D. Peng, F. Plasser, B. Pritchard, M. Reiher, I. Rivalta, I. Schapiro, J. Segarra-Martí, M. Stenrup, D. G. Truhlar, L. Ungur, A. Valentini, S. Vancoillie, V. Veryazov, V. P. Vysotskiy, O. Weingart, F. Zapata, and R. Lindh, J. Comput. Chem. **37**, 506 (2016).
[29] I. Fdez Galván *et al.*, J. Chem. Theory Comput. **15**, 5925 (2019).
[30] F. Aquilante *et al.*, J. Chem. Phys. **152**, 214117 (2020).
[31] B. O. Roos, R. Lindh, P.-Å. Malmqvist, V. Veryazov, and P.-O. Widmark, J. Phys. Chem. A **108**, 2851 (2004).
[32] B. O. Roos, R. Lindh, P.-Å. Malmqvist, V. Veryazov, and P.-O. Widmark, J. Phys. Chem. A **109**, 6575 (2005).
[33] I. F. Galván, M. G. Delcey, T. B. Pedersen, F. Aquilante, and R. Lindh, J. Chem. Theory Comput. **12**, 3636 (2016).
[34] V. Barone and M. Cossi, J. Phys. Chem. A **102**, 1995 (1998).
[35] M. Cossi, N. Rega, G. Scalmani, and V. Barone, J. Chem. Phys. **114**, 5691 (2001).
[36] P. Rademacher, R. Stølevik, and W. Lüttke, Angew. Chem., Int. Ed. Engl. **7**, 806 (1968).
[37] P. Rademacher and R. Stølevik, Acta Chem. Scand. **23**, 660 (1969).
[38] J. Soto, M. Algarra, and D. Peláez, Phys. Chem. Chem. Phys. **24**, 5109 (2022).
[39] J. Soto and M. Algarra, J. Phys. Chem. A **125**, 9431 (2021).
[40] J. Soto, F. J. Avila, J. C. Otero, and J. F. Arenas, Phys. Chem. Chem. Phys. **13**, 7230 (2011).
[41] C. Møller and M. S. Plesset, Phys. Rev. **46**, 618 (1934).
[42] F. Weigend and R. Ahlrichs, Phys. Chem. Chem. Phys. **7**, 3297 (2005).
[43] F. Weigend, Phys. Chem. Chem. Phys. **8**, 1057 (2006).
[44] A.-R. Allouche, J. Comput. Chem. **32**, 174 (2011).
[45] G. Schaftenaar and J. H. J. Noordik, J. Comput. Aided Mol. Design. **14**, 123 (2000).
[46] B. M. Bode and M. S. Gordon, J. Mol. Graphics Modell. **16**, 133 (1998).
[47] J. Soto, J. C. Otero, F. J. Avila, and D. Peláez, Phys. Chem. Chem. Phys. **21**, 2389 (2019).
[48] D. Aranda, F. J. Avila, I. López-Tocón, J. F. Arenas, J. C. Otero, and J. Soto, Phys. Chem. Chem. Phys. **20**, 7764 (2018).
[49] J. Soto, D. Peláez, J. C. Otero, F. J. Avila, and J. F. Arenas, Phys. Chem. Chem. Phys. **11**, 2631 (2009).
[50] J. F. Arenas, J. C. Otero, D. Peláez, and J. Soto, J. Phys. Chem. A **109**, 7172 (2005).
[51] L. J. Butler, Annu. Rev. Phys. Chem. **49**, 125 (1998).
[52] N. R. Forde, T. L. Myers, and L. J. Butler, Faraday Discuss. **108**, 221 (1997).
[53] G. C. G. Waschewsky, P. W. Kash, T. L. Myers, D. C. Kitchen, and L. J. Butler, J. Chem. Soc., Faraday Trans. **90**, 1581 (1994).

[54]L. Blancafort, P. Hunt, and M. A. Robb, J. Am. Chem. Soc. **127**, 3391 (2005).
[55]C. Ko, B. Levine, A. Toniolo, L. Manohar, S. Olsen, H.-J. Werner, and T. J. Martínez, J. Am. Chem. Soc. **125**, 12710 (2003).
[56]G. Chaban, M. S. Gordon, and D. R. Yarkony, J. Phys. Chem. A **101**, 7953 (1997).
[57]J. Soto, J. F. Arenas, J. C. Otero, and D. Peláez, J. Phys. Chem. A **110**, 8221 (2006).
[58]T. J. Martínez, Chem. Phys. Lett. **272**, 139 (1997).
[59]M. T. Anderson and F. Weinhold, Phys. Rev. A **10**, 1457 (1974).
[60]M. A. El-Sayed, J. Chem. Phys. **38**, 2834 (1963).
[61]J. Soto and J. C. Otero, J. Phys. Chem. A **123**, 9053 (2019).
[62]R. Bonneau, M. T. H. Liu, K. C. Kim, and J. L. Goodman, J. Am. Chem. Soc. **118**, 3829 (1996).
[63]X.-P. Chang, T.-S. Zhang, Y.-G. Fang, and G. Cui, J. Phys. Chem. A **125**, 1880 (2021).
[64]A. Fernández-Ramos, J. Rodríguez-Otero, M. A. Ríos, and J. Soto, J. Mol. Struct.: THEOCHEM **489**, 255 (1999).
[65]J. Soto, J. Phys. Chem. A **126**, 8372 (2022).
[66]E. B. Wilson, Jr., J. C. Decius, and P. C. Cross, *Molecular Vibrations* (McGraw-Hills, New York, 1955).
[67]J. F. Arenas, S. P. Centeno, J. I. Marcos, J. C. Otero, and J. Soto, J. Chem. Phys. **113**, 8472 (2000).